

Supplemental Information

**Tropomodulin Protects α -Catenin-Dependent
Junctional-Actin Networks under Stress
during Epithelial Morphogenesis**

Elisabeth A. Cox-Paulson, Elise Walck-Shannon, Allison M. Lynch, Sawako Yamashiro,
Ronen Zaidel-Bar, Celeste C. Eno, Shoichiro Ono, and Jeff Hardin

Table S1. Number and Directionality of Junctional Extensions in *hmp-1(fe4)* and *hmp-1(fe4);unc-94(RNAi)* Embryos

	# embryos analyzed	# total extensions (≥ 0.5 mm)	# non-seam directed extensions (≥ 0.5 mm)	# seam directed extensions (≥ 0.5 mm)
<i>hmp-1(fe4); jac-1::gfp</i>	21	48 (2.3 / embryo)	22 (1.0 / embryo)	26 (1.2 / embryo)
<i>hmp-1(fe4); jac-1::gfp; unc-94(RNAi)</i>	18	97 (5.4 / embryo)	60 (3.3 / embryo)	37 (2.1 / embryo)

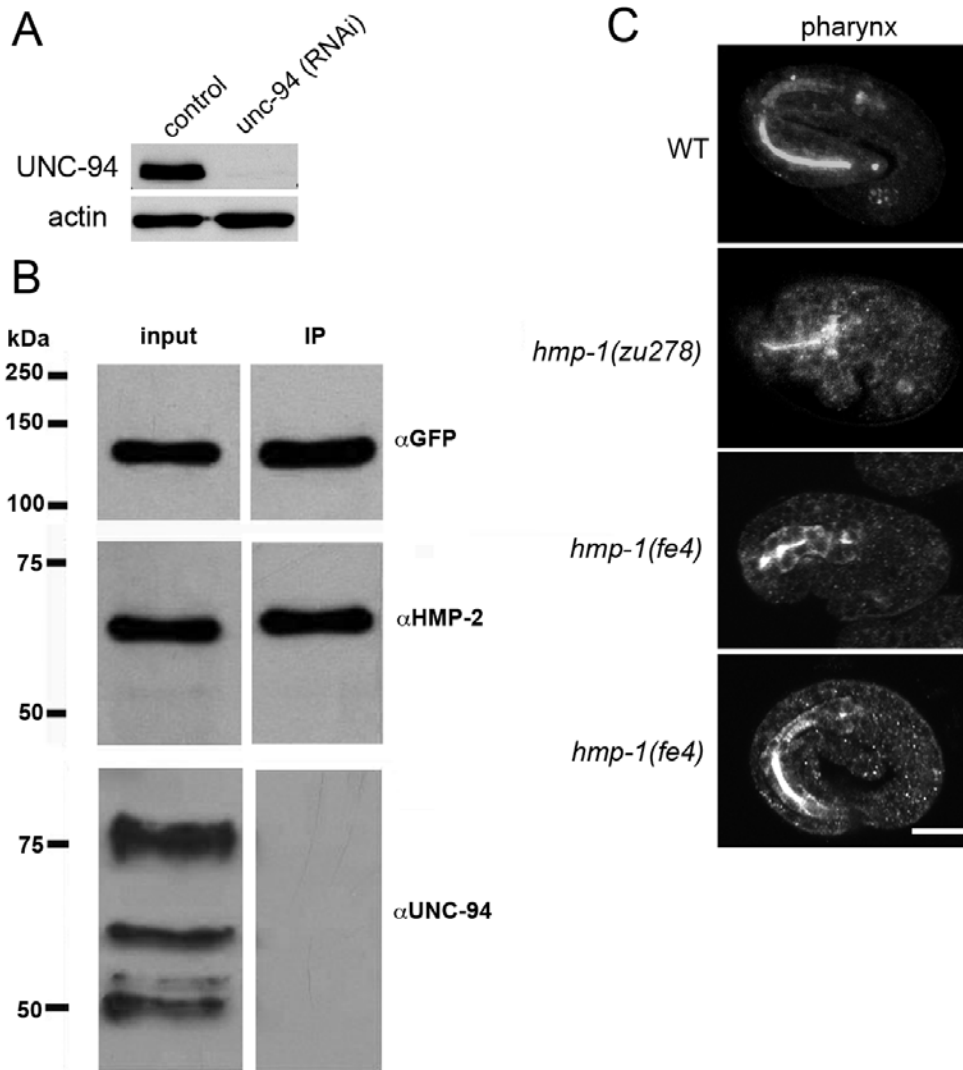


Figure S1. Additional Analysis of HMP-1 and UNC-94 Interactions

A. Western blot showing reduced expression of UNC-94 in *unc-94(RNAi)* embryos. Lysate from 30 N2 or N2; *unc-94(RNAi)* worms was loaded in each lane and probed for either UNC-94 or actin. Western blot showing reduced expression of UNC-94 in embryos treated with *unc-94(RNAi)*. Lysate from 30 N2 or N2; *unc-94(RNAi)* worms was loaded in each lane and probed for either UNC-94 or actin. RNAi was performed via feeding. B. HMP-1 and UNC-94 do not coimmunoprecipitate. SU265 (*hmp-1::gfp; dlg-1::dsRed*) embryos were collected and extracts collected as described in Experimental Procedures. Extracts were subjected to immunoprecipitation using anti-GFP antibodies, and the resulting non-precipitated proteins (input) and immunoprecipitates (IP) were blotted and probed using anti-GFP (α GFP), anti-HMP-2 (α HMP-2), or anti-UNC-94 (α UNC-94) antibodies. Whereas there is robust signal for HMP-1::GFP (top) or HMP-2, a known HMP-1 binding protein (middle) in the IP, there is no detectable UNC-94 (bottom), although there was abundant UNC-94 in the original extract (bottom, left). C. UNC-94 staining in the pharynx. In wild-type elongation-stage embryos, 100% show staining for UNC-94 in the pharynx (n = 79). In *hmp-1(zu278)* embryos, 86% have UNC-94 staining in the pharynx (n = 87). In *hmp-1(fe4)* embryos, 100% of elongating embryos show staining for UNC-94 in the pharynx (n = 63). Bar = 10 μ m.

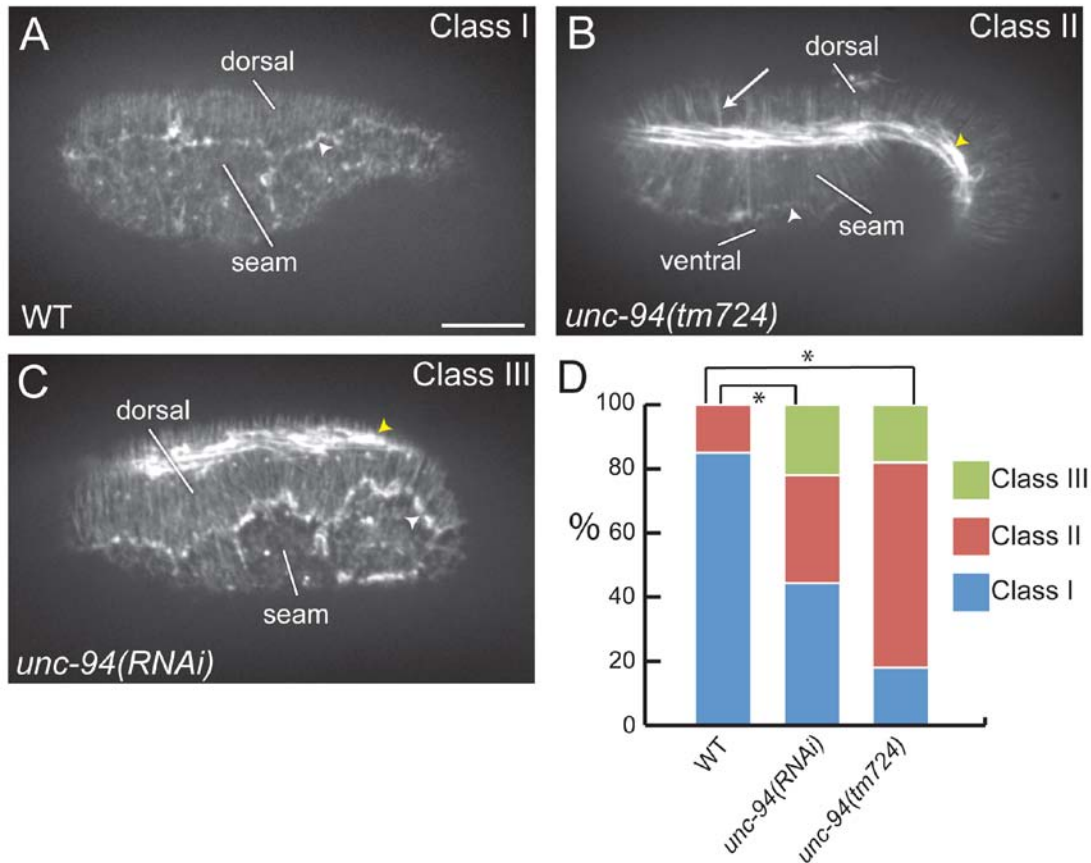


Figure S2. Junctional-Proximal Actin and Circumferential Filament Bundles (CFBs) Are Perturbed in *unc-94* Loss-of-Function Embryos

Phalloidin staining of actin in ~1.5-fold embryos. Phenotypic defects were categorized into three classes. (A) In Class I embryos (wild-type embryo shown), there is a clear thin band of actin at the junction (white arrowhead), evenly spaced CFBs, and a dense meshwork of actin in seam cells. (B) In Class II embryos (*unc-94(tm724)* embryo shown), there are clumps of CFBs (arrow), but the overall amount of actin in the embryo is not decreased. Muscle organization is also perturbed (yellow arrowhead). (C) In Class III embryos (*unc-94(RNAi)* embryo shown), there is clumping of junctional actin and often a substantial decrease in the amount of actin present in seam cells (not visible in this example). As in Class II embryos, muscle organization is perturbed (yellow arrowhead). (D) Distribution of phenotypes for the three genotypes of embryos screened (wildtype, n=13; *unc-94(RNAi)*, n=19; *unc-94(tm724)* n=11). For all images, anterior is to the left; bar=10µm. * = significantly different, p < 0.05. *unc-94(RNAi)* and *unc-94(tm724)* are not significantly different (p = 0.32).

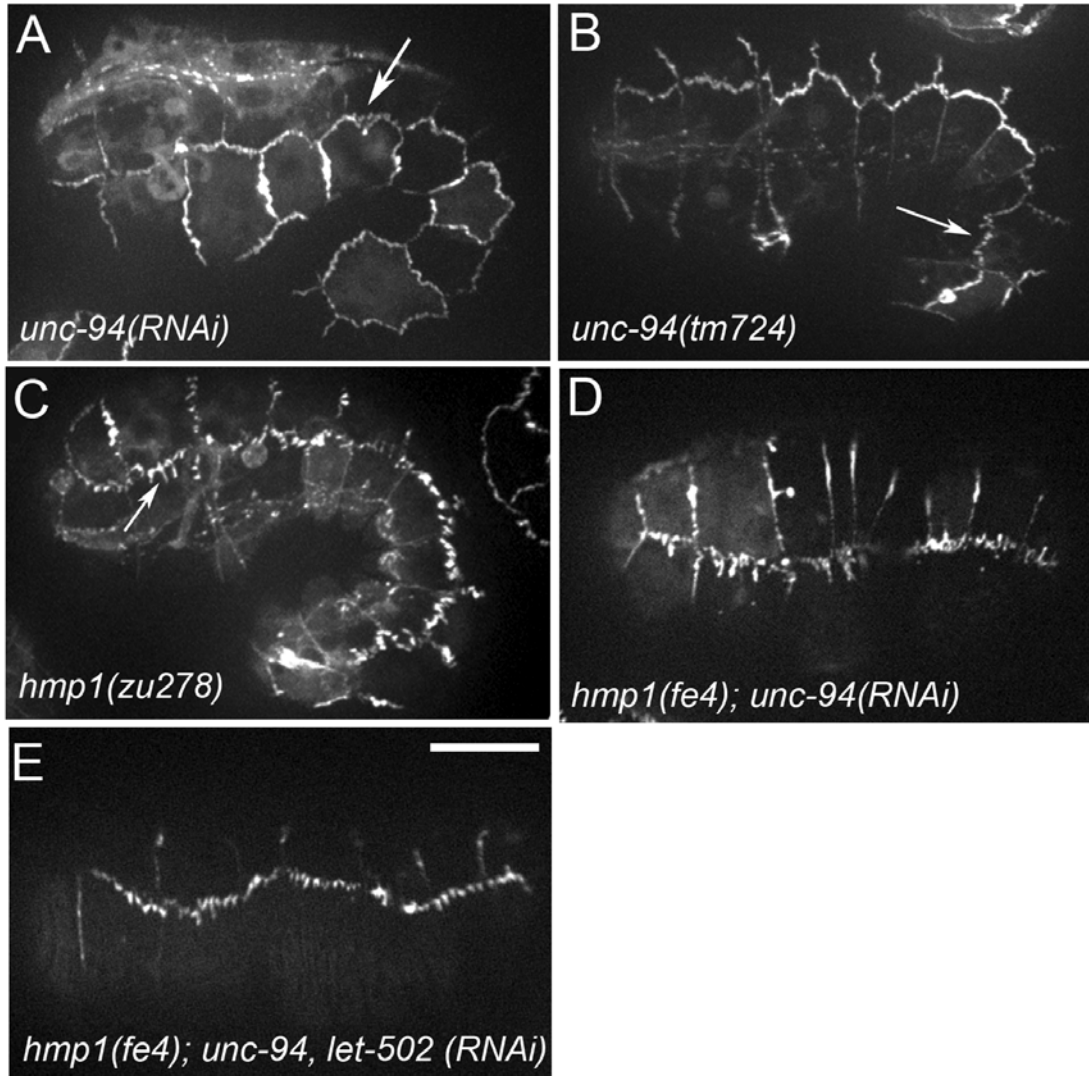


Figure S3. The Adherens Junctions of *hmp-1(fe4);unc-94(RNAi)* Embryos Exhibit Abnormal Dynamics in Living Embryos

JAC-1::GFP localization was assessed in living embryos using spinning disc confocal microscopy. (A, B) *unc-94* loss-of-function results in slightly perturbed adherens junctions. (A) *unc-94(RNAi)* embryo. Regions of JAC-1::GFP mislocalization (arrow), were observed in 3 out of 23 embryos examined. (B) *unc-94(tm724)* embryo. (C) *hmp-1(zu278)* embryo. In 6 out of 6 embryos observed (at the 1.25-1.5 fold stage), the seam:ventral/seam:dorsal borders exhibited dislocation of JAC-1::GFP reminiscent of, but not quite as dynamic as, that seen in *hmp-1(fe4);unc-94(RNAi)* embryos. (D, E) *let-502(RNAi)* ameliorates the junctional dislocation in *hmp-1(fe4);unc-94(RNAi)* embryos. (D) Arrested *hmp-1(fe4);unc-94(RNAi)* embryo showing dislocated JAC-1::GFP. (E) Arrested *hmp-1(fe4);unc-94, let-502(RNAi)* embryo. Some regions in C and D are slightly out of focus due to the shape of the embryos and movement due to muscle twitching. Bar = 10 μ m.

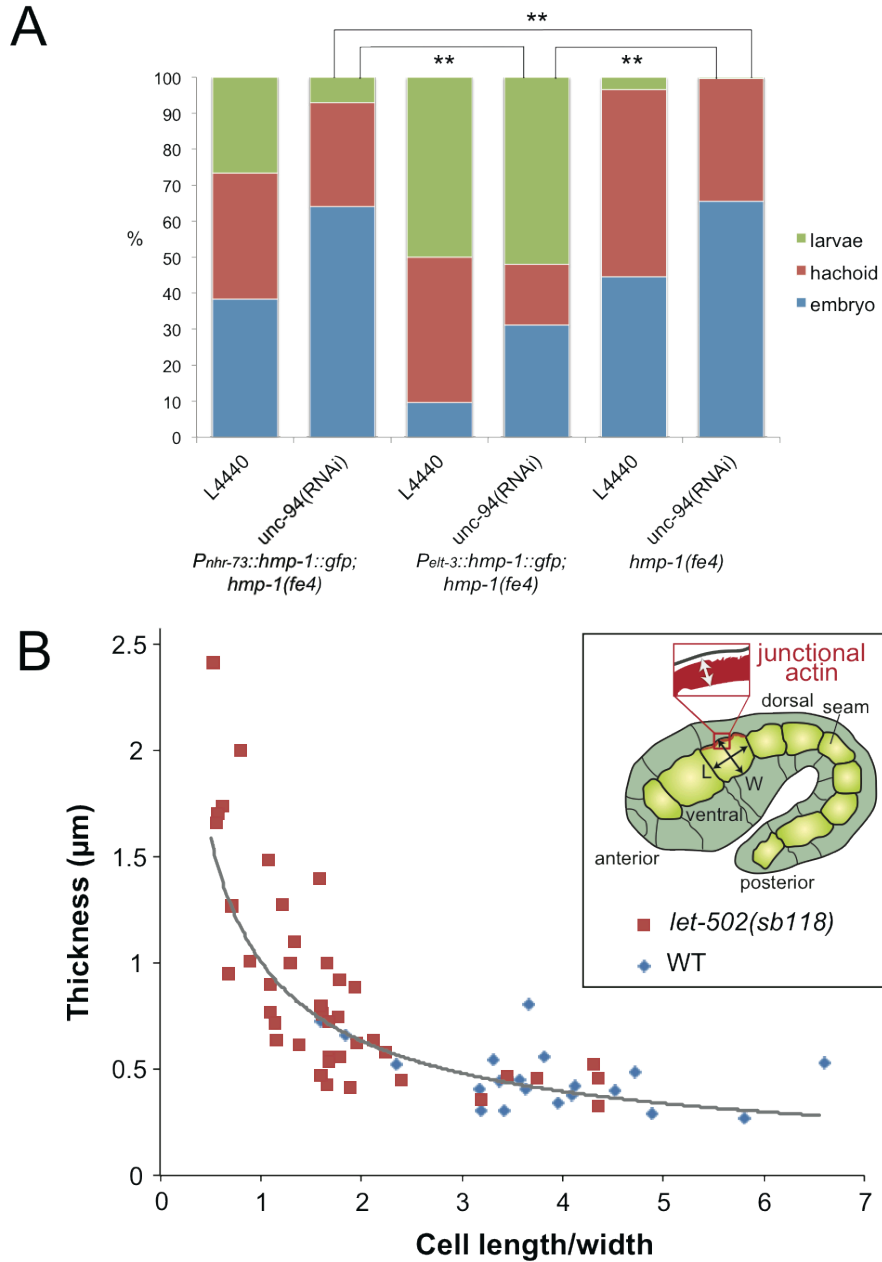


Figure S4. Tissue-Specific Requirements for HMP-1 and UNC-94 Function and Effects of LET-502/ROCK on Junctional-Proximal Actin

A. Tissue-specific rescue of defects in *hmp-1(fe4);unc-94(RNAi)* embryos indicates a major requirement for HMP-1 and UNC-94 in non-seam epidermal cells. *hmp-1(fe4)* hermaphrodites expressing *Pnhr-73::hmp-1::gfp* (expressed in seam cells) or *Pelt-3::hmp-1::gfp* (expressed in non-seam cells) were subjected to *unc-94(RNAi)* via feeding or fed control bacteria (L4440), and progeny scored for developmental arrest. ** = significantly different, $p < 0.001$. B. Loss of *let-502/Rho* kinase function leads to shorter cells with thicker UNC-94-positive junctional proximal actin bands. *let-502(sb118)* embryos were temperature-shifted as described in Experimental Procedures and immunostained for AJM-1(to determine overall cell shape) and UNC-94. The thickness of the UNC-94-containing junctional proximal band was measured as shown and plotted against length/width ratio for *let-502(sb118)* and wild-type embryos. A power curve was used to fit the resulting data.

Supplemental Experimental Procedures

Strains and Alleles

The Bristol N2 strain was used as wildtype. *hmp-1(fe4)* [1] was maintained as a heterozygote over *lon-3(e2175)* as a marker for the wild-type chromosome. The previously described *jac-1::gfp* transgene [1] was integrated via gamma irradiation (*jcIs24*), outcrossed six times, and homozygosed to generate the strain SU295. Crosses were performed to introduce *jcIs24* into *hmp-1(fe4)/lon-3(e2175)* and into *unc-94(tm724)*. *unc-94(tm724)* was obtained from Shohei Mitani (National Bioresource Project for *C. elegans*, Tokyo Women's Medical University School of Medicine, Tokyo, Japan). The *unc-94(tm724)* allele has a 695 base pair deletion and 17 bp insertion that might result in a frame shift after the third exon.

A strain (ML753) expressing a *gfp*-tagged fragment of *vab-10* that binds F-actin in epidermal cells (VAB-10(ABD):GFP [2]) was mated with *unc-94(tm724)* or *hmp-1(fe4)* males and the relevant mutation was rehomozygosed to create strains used in spinning disc confocal filming experiments.

HR1157 carries a *let-502* temperature sensitive allele (*sb118*) that was kindly provided by Paul Mains (University of Calgary).

Tissue-specific HMP-1 rescuing constructs were made using Fusion PCR [3]. The *nhr-73* promoter was used for seam-specific expression and the *elt-3* promoter was used for non-seam epidermal expression. Phusion Polymerase (NEB) was used to PCR amplify ~1kb of the *nhr-73* promoter (5' CTTGAGCAACAATTTTCAGAGCAGTGGAGGTTTTGT3' forward and 3' CCATTCGCAGGCAT TCTGAAAATTAATTTTTCTTCAAACCTTGCC5' reverse, with 25bp overhang for *hmp-1*) or ~2kb of the *elt-3* promoter (5' ACCGAAATGCCGATGGACATATCAAATGTGAAGACA3' and 3' CATGAGAATTGCCATTCGCAGGCATGAAGTTTGAAATACCAGGTAGCCGA5' reverse, with 25bp overhang for *hmp-1*) from *C. elegans* genomic DNA. *hmp-1::gfp* was PCR amplified using Phusion Polymerase with pJS434 [4] as a template (5' TAATTTTCAGAATGCCTGCGAATGG3' forward and 3' GCATAGTTAAGCCAGCCCCGACACC5' reverse) for fusion to *P_{nhr-73}* or 5' ATGTGTCAGAGGTTTTACCGTCAT3' forward and 3' ATGTGTCAGAGGTTTTACCGTCAT5' reverse for fusion to *P_{elt-3}*). Fusion PCR was performed to connect these two nested PCR products using *Go Taq Long* (for *P_{nhr-73}::hmp-1::gfp*: 5' TATGTGTCAGAGGTTTTACCGTCAT3' and 3' ATGTGTCAGAGGTTTTACCGTCAT5'; for *P_{elt-3}::hmp-1::gfp*: 5' GTTTCTACTGTTTCAACATTATGTGTCAGAGGTTTTACCGTCAT3' and 3' ATGTGTCAGAGGTTTTACCGTCAT5').

Fusion PCR constructs (*P_{elt-3}::hmp-1::gfp* and *P_{nhr-73}::hmp-1::gfp*) were injected into *hmp-1(fe4)* worms. At least two reactions were pooled for injection to minimize the chance of proofreading

errors. About 80ng of the Fusion reactions were co-injected with *P_{ttx-3}::dsRed* into the gonads of *hmp-1(fe4)* worms. Expression of the HMP-1::GFP constructs in either seam or non-seam cells was verified with confocal microscopy.

Antibodies

A polyclonal rabbit anti-UNC-94 antibody was produced and affinity purified by the Proteintech Group, Inc. (Chicago, IL) using amino acids 144-401 of UNC-94b as the antigen as previously described [5]. Rabbit anti-HMR-1 antibody was generously provided by J. Priess (Fred Hutchinson Cancer Research Center, Seattle, WA). MH27 antibodies were purified from ascites fluid (Harlan Sprague Dawley, Madison, WI) from hybridoma cells obtained from the Developmental Hybridoma Bank (Univ. of Iowa). A monoclonal anti-actin antibody (C4, MP Biomedicals, Irvine CA) was used for Western blotting.

Feeding RNAi Screening

The *C. elegans* Chromosome I feeding RNAi library in 96 well format was used for screening [6]. This library contains 2,445 bacterial cultures (HT115 (DE3) strain) each expressing a unique feeding RNAi clone. A starter culture (LB with 25 µg/mL carbenicillin and 12.5 µg/mL tetracycline) was inoculated with a replicator tool, using frozen material from the library plates, and grown overnight at 37°C. A second culture (LB + 25 µg/mL carbenicillin) was inoculated using material from the starter plate and cultured overnight at 37°C. 10 µL of this culture was spread onto triplicate wells of 12 well plates containing Nematode Growth Media [7] supplemented with 25 µg/mL carbenicillin and 1mM isopropyl β-D-thiogalactopyranoside (IPTG). The bacteria were grown overnight to generate a thin lawn.

Approximately 20-30 L3-L4 *hmp-1(fe4)* worms were seeded onto one well for each clone to be tested. After allowing the worms to feed for 24 hours, 8 were singled onto each of the two remaining wells for each clone. After another 24 hours, the worms were removed from the plates. Over the next two days, the wells were visually scanned to determine the approximate percentage of embryonic lethality. Feeding RNAi for wild type worms was performed in a similar manner except that 10-15 worms were seeded in the initial well and four were singled into the duplicate wells. In each round of the screen, *hmp-1(fe4)* worms were fed the empty feeding vector, L4440[8], as a negative control and a feeding vector for the known *hmp-1(fe4)* enhancer, *unc-34* [9] as a positive control.

We identified 44 transcription units that, when depleted with feeding RNAi, enhanced the lethality of *hmp-1(fe4)* to 95% or greater, and yielded less than 12% lethality in wild-type. A

secondary screen was performed to confirm putative enhancers using a different source of double-stranded RNA (dsRNA) and RNAi by injection.

RNAi via Injection and Dead Embryo Counts

dsRNA was injected at 2 $\mu\text{g}/\mu\text{l}$ into one gonad arm per worm, with the exception of *let-502(RNAi)*, which was injected at 1 $\mu\text{g}/\mu\text{l}$ to avoid early arrest due to cytokinesis defects. To score for embryonic and early larval lethality, worms were cultured for 12-16 hours after injection and then singled onto new plates. The embryos produced over the next 24 hours were scored for lethality. To obtain embryos for phenotypic analysis, worms were cut transversely through the vulva at 24 - 30 hours post-injection and extruded embryos were collected.

For tissue-specific rescue experiments, worms were selected for application to either empty vector (L4440) or *tmd-1* feeding RNAi plates based on the dsRed signal. Lethality was counted after 48 hours of feeding. Chi-square analysis was performed using the online contingency table form available at <http://www.physics.csbsju.edu/stats/contingency.html>.

Morphological Analysis and Embryo Staining

4D Nomarski microscopy was performed as described previously [10]. Phalloidin staining was performed using a modification of a previously described protocol [11]. Briefly, embryos were placed on poly-L-lysine coated slides, aged, treated with 1 mg/ml chitinase in egg salts for 20 min., and fixed with a solution of 4% paraformaldehyde, 0.1 mg/mL lysolecithin, 10 mM EGTA, 48 mM PIPES (pH 6.8), 25 mM HEPES (pH 6.8) and 2 mM MgCl_2 . Embryos were stained with 1:20 Alexa555-phalloidin (Invitrogen Corp., Carlsbad, CA) overnight at 4°C. For immunostaining, embryos were freeze cracked and stained as described [12].

For immunocytochemistry experiments and live imaging of JAC-1::GFP and VAB-10(ABD)::GFP, embryos were observed using a Perkin Elmer Ultraview spinning disk confocal microscope and processed as described [9]. For videos of JAC-1::GFP, stacks of images (12-16 sections/stack) were taken at 10 sec intervals for 5 min; for VAB-10(ABD)::GFP, 10-30 focal planes were captured at 30-120 sec intervals. Some images shown are projections of multiple focal planes. Cells in elongating *vab-10(ABD)::gfp* embryos at the comma stage were scored as having discontinuous actin bands if no discernible accumulation of actin could be identified over > 50% of their ventral perimeter.

Actin defects in phalloidin stained specimens were scored as follows. Stained ~1.5-fold embryos were categorized into three classes. In class I embryos a clear, thin band of actin at the junction and evenly spaced circumferential filaments bundles (CFBs) were apparent, along with a dense meshwork

of actin in seam cells. In class II embryos, clumps of CFBs were visible, but the overall amount of actin in the embryo was not decreased. In class III embryos, clumping of junctional actin occurred, and there was a substantial decrease in the amount of actin present in seam cells. Embryos were categorized by three independent assessors and the results compiled. Chi-square analysis was performed as above (see Procedures for tissue-specific rescue).

For measuring continuity of junctional proximal actin networks, a 5 pixel-wide freehand selection was hand-traced along individual cell-cell junctions from maximum-intensity Z stack projections of phalloidin stained specimens. The selection was then straightened using the “Edit->Selection->Straighten...” command in ImageJ. The signal was manually thresholded for each selection using the “Image->Adjust->Threshold...” command to include all visible fluorescence along the straightened cell-cell boundary. The number, size and total area of thresholded particles was then calculated using the “Analyze->Analyze Particles...” command in ImageJ. Since the variances of the wild-type and experimental groups failed the F test, pairwise heteroscedastic T-tests were performed using Excel and StatPlus:mac (AnalystSoft). To construct box plots, standard box plot conventions were used. The first (Q1) and third (Q3) quartiles, interquartile range ($IQR = Q3 - Q1$) and mean were calculated. Extreme outliers were defined as lying beyond the outer fences $OF1 = Q1 - 3 * IQR$ and $OF2 = Q3 + 3 * IQR$. Mild outliers were defined as lying between $OF1$ and $Q1 - 1.5 * IQR$ or $OF2$ and $Q3 + 1.5 * IQR$. Box plots were constructed using StatPlus:mac.

For analysis of *let-502(ts)* embryos, worms carrying embryos were shifted to an intermediate, restrictive temperature (25.5°C) and grown overnight. Embryos were recovered, stained via freeze-cracking [10] using MH27 and anti-UNC-94 antibodies and appropriate secondary antibodies (1:50 α -rabbit-FITC, 1:50 α -mouse-Texas Red), and imaged using spinning disc confocal microscopy. The thickness of the junctional proximal actin at dorsal::seam boundaries was measured at several points along the perimeter of individual cells using ImageJ (available at <http://rsbweb.nih.gov/ij/>), and an average thickness was calculated for each cell measured. The length/width ratio of each cell was also measured in ImageJ using the AJM-1 signal. The resulting actin band thickness vs. length/width data were plotted in Excel and a curve fit was obtained using a power law.

Coimmunoprecipitation Assays

Embryos were collected from 10 large plates grown for 3-4 days at 20°C, homogenized in Lysis buffer + 0.25% Triton X-100, subjected to centrifugation to clear the lysates, and precleared by incubation on ice with 20 μ l of a 50% slurry of Protein G-Agarose beads essentially as described [13, 14]. To perform IPs, 5 μ l E36 mouse monoclonal anti-GFP (Invitrogen) was added to pre-cleared lysate and rotated at 4°C for 1 hour, 40 μ l of 50% prepared Protein G-Agarose bead slurry (Pierce)

was added, and rotated again at 4°C for 1 hour. Beads were sedimented at 3000 rpm for 3 min (4°C), washed 3X with Lysis buffer, and 25ul 4x SDS-PAGE sample buffer was then added to preclear, prewash, and IP bead fractions on ice. Collected samples were then subjected to SDS-PAGE on an 8% gel, along with 10 µl of Precision Plus Kaleidoscope Standard (Bio-Rad), and blotted onto PVDF membrane. Blots were blocked using TBST + 5% non-fat dry milk, incubated in 1:2500 primary (anti-UNC-94) antibody, washed in TBST, incubated in 1:10,000 anti-Rabbit HRP conjugate, and visualized using enhanced chemiluminescence (ECL; Pierce) on X-ray film.

Expression and Purification of Recombinant UNC-94 Protein

A full-length *unc-94b* cDNA was cloned into plasmid pKLD37 using a vector provided by I. Rayment (Dept. of Biochemistry, Univ. of Wisconsin), which consisted of pET31b with an N-term 6His-rTEV site. The *Escherichia coli* strain BL21 (DE3) was transformed with the expression vector and cultured in M9ZB medium (Novagen, EMD Biosciences, Inc., San Diego, CA) containing 50 µg/ml ampicillin at 37 °C until A_{600} reached 0.6 cm⁻¹. Protein expression was induced by adding 0.4 mM IPTG for 3 hours. The cells were harvested by centrifugation at 5,000 g for 10 minutes and disrupted by a French Pressure cell at 360-580 kg/cm² in a buffer containing 0.3 M NaCl, 50 mM NaPO₄, 10 mM imidazole, 1 mM phenylmethanesulfonyl fluoride, pH 7.4. The homogenates were centrifuged at 20,000 g and the supernatants applied to a TALON cobalt affinity column (Clontech, Mountain View, CA). Bound proteins were eluted with 0.3 M NaCl, 50 mM NaPO₄, 100 mM imidazole, pH 7.4. The fractions containing UNC-94 were dialyzed against 10 mM PIPES, 0.2 mM dithiothreitol, pH 7.0 and purified further with a Mono-Q column (Amersham Biosciences, GE Healthcare Bio-sciences, Corp., Piscataway, NJ) by elution with a linear NaCl gradient (0.1-0.5 M). Fractions containing purified UNC-94 were dialyzed against F-buffer (0.1 M KCl, 2 mM MgCl₂, 1 mM dithiothreitol, 20 mM Hepes-NaOH, pH 7.5). Concentrations of UNC-94 were determined by densitometry of Coomassie blue-stained protein bands after SDS-PAGE using actin as a standard.

Actin Bundling Assays

Recombinant UNC-94 was expressed and purified as described above. GST-tagged HMP-1 was produced using constructs previously described [4], purified on glutathione beads, eluted with 10 mM glutathione, and cleaved with TEV protease in 50 mM Tris, pH 8 in solution. The digest was purified using a Sephacryl S-300 column. Rabbit muscle G-actin (20% labeled with DyLight549) [15] was polymerized in the presence of chicken CapZ [16] at a 100:1 molar ratio. Filaments were diluted to 5 µM actin with or without 5 µM HMP-1 and 2.5 µM UNC-94 and incubated for 15 min, mounted on nitrocellulose-coated coverslips, and observed by epifluorescence using a Nikon TE2000 inverted

microscope. The curvilinear lengths of resulting bundles were measured using the NeuronJ plugin for ImageJ, available at <http://rsbweb.nih.gov/ij/>. Statistics were performed using Excel and StatPlus:Mac.

Supplemental References

1. Pettitt, J., Cox, E.A., Broadbent, I.D., Flett, A., and Hardin, J. (2003). The *Caenorhabditis elegans* p120 catenin homologue, JAC-1, modulates cadherin-catenin function during epidermal morphogenesis. *J Cell Biol* *162*, 15-22.
2. Diogon, M., Wissler, F., Quintin, S., Nagamatsu, Y., Sookhareea, S., Landmann, F., Hutter, H., Vitale, N., and Labouesse, M. (2007). The RhoGAP RGA-2 and LET-502/ROCK achieve a balance of actomyosin-dependent forces in *C. elegans* epidermis to control morphogenesis. *Development* *134*, 2469-2479.
3. Boulin, T., Etchberger, J.F., and Hobert, O. (2006). Reporter gene fusions. *WormBook*, 1-23.
4. Kwiatkowski, A.V., Maiden, S.L., Pokutta, S., Choi, H.J., Benjamin, J.M., Lynch, A.M., Nelson, W.J., Weis, W.I., and Hardin, J. (2010). In vitro and in vivo reconstitution of the cadherin-catenin-actin complex from *Caenorhabditis elegans*. *Proc Natl Acad Sci U S A* *107*, 14591-14596.
5. Stevenson, T.O., Mercer, K.B., Cox, E.A., Szewczyk, N.J., Conley, C.A., Hardin, J.D., and Benian, G.M. (2007). *unc-94* encodes a tropomodulin in *Caenorhabditis elegans*. *Journal of molecular biology* *374*, 936-950.
6. Fraser, A.G., Kamath, R.S., Zipperlen, P., Martinez-Campos, M., Sohrmann, M., and Ahringer, J. (2000). Functional genomic analysis of *C. elegans* chromosome I by systematic RNA interference. *Nature* *408*, 325-330.
7. Brenner, S. (1974). The genetics of *Caenorhabditis elegans*. *Genetics* *77*, 71-94.
8. Timmons, L., and Fire, A. (1998). Specific interference by ingested dsRNA. *Nature* *395*, 854.
9. Sheffield, M., Loveless, T., Hardin, J., and Pettitt, J. (2007). *C. elegans* Enabled exhibits novel interactions with N-WASP, Abl, and cell-cell junctions. *Curr Biol* *17*, 1791-1796.
10. Williams-Masson, E.M., Malik, A.N., and Hardin, J. (1997). An actin-mediated two-step mechanism is required for ventral enclosure of the *C. elegans* hypodermis. *Development* *124*, 2889-2901.
11. Costa, M., Raich, W., Agbunag, C., Leung, B., Hardin, J., and Priess, J.R. (1998). A putative catenin-cadherin system mediates morphogenesis of the *Caenorhabditis elegans* embryo. *J Cell Biol* *141*, 297-308.
12. Simske, J.S., Koppen, M., Sims, P., Hodgkin, J., Yonkof, A., and Hardin, J. (2003). The cell junction protein VAB-9 regulates adhesion and epidermal morphology in *C. elegans*. *Nat Cell Biol* *5*, 619-625.
13. Bernadskaya, Y.Y., Patel, F.B., Hsu, H.T., and Soto, M.C. (2011). Arp2/3 promotes junction formation and maintenance in the *Caenorhabditis elegans* intestine by regulating membrane association of apical proteins. *Molecular biology of the cell* *22*, 2886-2899.
14. Giuliani, C., Troglio, F., Bai, Z., Patel, F.B., Zucconi, A., Malabarba, M.G., Dianza, A., Stradal, T.B., Cassata, G., Confalonieri, S., et al. (2009). Requirements for F-BAR proteins TOCA-1 and TOCA-2 in actin dynamics and membrane trafficking during *Caenorhabditis elegans* oocyte growth and embryonic epidermal morphogenesis. *PLoS genetics* *5*, e1000675.
15. Liu, Z., Klaavuniemi, T., and Ono, S. (2010). Distinct roles of four gelsolin-like domains of *Caenorhabditis elegans* gelsolin-like protein-1 in actin filament severing, barbed end capping, and phosphoinositide binding. *Biochemistry* *49*, 4349-4360.
16. Soeno, Y., Abe, H., Kimura, S., Maruyama, K., and Obinata, T. (1998). Generation of functional beta-actinin (CapZ) in an *E. coli* expression system. *J Muscle Res Cell Motil* *19*, 639-646.